Langmuir

Article

pubs.acs.org/Langmuir

Simplifying the Evaluation of Graphene Modified Electrode Performance Using Rotating Disk Electrode Voltammetry

Si-Xuan Guo,[†] Shu-Feng Zhao,[†,‡] Alan M. Bond,*[,†] and Jie Zhang*[,†]

[†]School of Chemistry, Monash University, Clayton, Vic 3800, Australia

[‡]Shanghai Key Laboratory of Green Chemistry and Chemical Processes, Department of Chemistry, East China Normal University, Shanghai 200062, P. R. China

Supporting Information

ABSTRACT: Graphene modified electrodes have been fabricated by electrodeposition from an aqueous graphene oxide solution onto conducting Pt, Au, glassy carbon, and indium tin dioxide substrates. Detailed investigations of the electrochemistry of the $[Ru(NH_3)_6]^{3+/2+}$ and $[Fe(CN)_6]^{3-/4-}$ and hydroquinone and uric acid oxidation processes have been undertaken at glassy carbon and graphene modified glassy carbon electrodes using transient cyclic voltammetry at a stationary electrode and near steady-state voltammetry at a rotating disk electrode. Comparisons of the data with simulation suggest that the transient voltammetric characteristics at graphene modified electrodes contain a significant contribution from thin layer and surface confined processes. Consequently, interpretations based solely on mass transport by semi-infinite linear diffusion may result in incorrect conclusions on the activity of the graphene modified electrode. In contrast, steady-state voltammetry at a rotating disk electrode affords a much simpler method for the evaluation of the performance of graphene modified electrode since the relative importance of the thin layer and surface confined processes are substantially diminished and mass transport is dominated by convection. Application of the rotated electrode approach with carbon nanotube modified electrodes also should lead to simplification of data analysis in this environment.

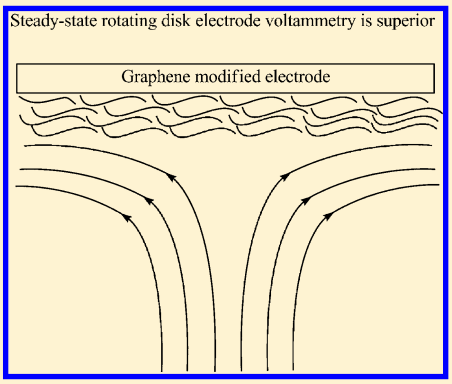

INTRODUCTION

Graphene is the latest member of the carbon family. It is an ideal two-dimensional nanomaterial which contains a sheet of carbon atoms bonded together with sp^2 bonds in a honeycomb-style lattice pattern.[1] Practically, multilayer carbon sheets (up to 10 layers) are also called graphene since their properties are close to those of single layer carbon sheet.[2] Since first reported by Geim and co-workers in 2004,[3] graphene has attracted great attention in many fields due to substantial fundamental and applied significance.

In contrast to carbon nanotubes that also have been of wide recent interest, graphene can be generated economically and conveniently via wet chemical methods, such as mechanical exfoliation, chemical vapor deposition,[2] and solvothermal synthesis.[4] Similar to other carbon based materials, graphene is highly stable and conductive, making it potentially attractive for electrochemical applications. In the area of electroanalytical chemistry, graphene modified electrodes have been widely evaluated for sensing applications.[5] Although graphene may be an ideal electrode material on the basis of advantages such as low cost, high electrical conductivity, and high stability, it is extremely difficult to fabricate a modified electrode consisting of a totally flat, defect-free, and single layer of graphene. For this practical reason, graphene modified electrodes used for most studies consist of multilayers of submicrometer-sized graphene sheets on a conventional conducting electrode substrate, such as a millimeter-diameter glassy carbon disk, except in the case of the recent study by Abruña and co-workers,[6] who did indeed prepare a monolayer of graphene electrode using microfabrication techniques.

Graphene modified electrodes are normally fabricated by one of two methods. The first involves direct deposition of graphene onto a conductive substrate by drop casting[7] or adsorption of graphene.[8] The second involves electrochemical reduction of graphene oxide to graphene, either from a graphene oxide film on the electrode surface[9] or from a solution containing dissolved graphene oxide.[10] The latter method has the advantage of producing a relatively uniform graphene layer with controllable thickness. Based on the results reported to date, it has been suggested that graphene represents a promising material for electroanalytical applications due to its high electrical conductivity and ability to promote rapid electron transfer.[5] However, it should be noted that recent studies by Goh and Pumera[11] suggest that graphene modified electrodes do not provide significant advantages over graphite microparticle modified electrodes for electroanalytical applications in terms of either sensitivity or reproducibility.

Excellent electrochemical performance has been attributed to the high density of edge-plane-like sites or defects in graphene

Received: December 20, 2011
Revised: February 12, 2012
Published: February 21, 2012

and a density of state argument,[12] which also is said to apply to carbon nanotubes.[13] Studies by Pumera et al.[14−16] suggested that the presence of oxygen containing functional groups also may affect the activity of graphene modified electrodes. The conclusion of high electrochemical activity of graphene has been reached largely on the basis of observation of small peak-to-peak separations, low overpotentials, and large currents detected in transient cyclic voltammograms, and assuming that theories based on the semi-infinite linear diffusion mass transport model are applicable.

The above-mentioned methods used for graphene modified electrode fabrication, although simple, invariably lead to the formation of stacks of multilayered graphene on the electrode surface. As a consequence, their characterization using transient voltammetry and interpretation of data via the theories based on mass transport by semi-infinite linear diffusion is problematic and may lead to incorrect conclusions with respect to the activity of graphene modified electrodes as has been shown to apply at carbon nanotube modified electrodes.[17] First, graphene films on the electrode surface are not dense. Thus, thin layer type processes[18] may be anticipated from the presence of analyte confined within the graphene layers, as found in the case of carbon nanotube modified electrodes.[17,19] Second, since graphene is electrically conductive and the surface is rough, the active area of the electrode can be significantly larger than the geometric area after modification with graphene. The graphene modified electrode configuration also favors adsorption which may contribute to the voltammetric response. Third, if the drop-coating method is used to fabricate the modified electrode, then the surface may not be fully covered by graphene. In this situation, electrochemistry will also occur at the underlying conductive substrate, resulting in mixed voltammetric responses from both graphene and the substrate. Finally, the capacitance of graphene is likely to be higher than that of the substrate, so that a larger unwanted background charging current and hence a relatively unfavorable faradaic-to-background current ratio is expected with a graphene modified electrode.

In principle, most of the above-mentioned nonidealities, except for the contribution from the underlying substrate electrode, but including the larger capacitance current highlighted above, can be minimized, made relatively unimportant, or even avoided if voltammetric experiments are conducted under steady-state rather than transient conditions. In this study, the reversible $[Ru(NH_3)_6]^{3+/2+}$ and quasi-reversible $[Fe(CN)_6]^{3-/4-}$ processes,[20,21] hydroquinone oxidation (a widely studied biologically important substance which undergoes a complex overall two-proton two-electron transfer reactions in aqueous media[22]), and uric acid oxidation (a widely studied biologically important substance which undergoes a chemically irreversible electrochemical process[23]) have been studied in detail using a graphene modified electrode fabricated by electrodeposition from graphene oxide. Both transient and near-steady-state (rotating disk electrode (RDE)) conditions have been employed in order to evaluate and compare the electrochemical performance of a graphene modified electrode under both sets of conditions. All of these processes examined have been studied at graphene modified electrodes by other research groups using transient cyclic voltammetry,[5] but not by the RDE method.

EXPERIMENTAL SECTION

Chemicals. Ruthenium hexamine trichloride ($[Ru(NH_3)_6]Cl_3$), potassium ferricyanide ($K_3[Fe(CN)_6]$), hydroquinone and uric acid (Sigma−Aldrich), Na_2HPO_4 and NaH_2PO_4 (Fluka, AR grade), HCl (AR grade, Univar), and KCl (Aldrich) were used as received from the manufacturer. Deionized water from a Milli-Q-MilliRho purification system (resistivity 18 M Ω cm) was used to prepare all aqueous electrolyte solutions. Buffer solutions were prepared by adding 0.1 M Na_2HPO_4 to the 0.1 M NaH_2PO_4 solution, and adjusting the pH to the desired value which was measured using a Metrohm 744 pH meter, equipped with a Metrohm 6.2306.020 glass electrode (Metrohm, Herisau, Switzerland).

Graphene oxide (GO) was synthesized from natural graphite (crystalline, 300 mesh, Alfa Aesar) using the method described by Hummers et al.[24]

Indium tin oxide (ITO) coated glass slides (surface resistivity: 8−12 Ω per sq, Aldrich) were treated using a literature method before use as electrodes.[25]

Electrodeposition of Graphene from Graphene Oxide. The electrodeposition of graphene from graphene oxide was achieved by methods similar to those reported by Chen et al.[10] In our method, the potential of the working electrode (glassy carbon, Au, Pt or ITO) was cycled between 0 and −1.4 V vs Ag/AgCl (3 M NaCl) to reduce graphene oxide using a scan rate of 0.05 V s^{-1} in an aqueous solution containing 1 mg mL^{-1} of graphene oxide and 0.05 M Na_2HPO_4. The electrogenerated graphene aggregates and deposits onto the electrode surface. To enhance the deposition rate, the solution was magnetically stirred. Alternatively, graphene modified electrodes were fabricated by electrodeposition of graphene from graphene oxide solution by cycling the potential for 10 cycles between 0 and −1.4 V vs Ag/AgCl (3 M NaCl) at a GC RDE working electrode at a rotation rate of 104.7 rad s^{-1} and a scan rate of 0.05 V s^{-1}. When the graphene film was deposited under hydrodynamic conditions, loosely attached graphene layers would not remain adhered to the electrode surface. Two variations of graphene modified electrodes were employed in the voltammetric studies: (a) wet graphene modified electrodes: after electrodeposition, electrodes were rinsed with distilled water several times and used directly without drying; (b) dried graphene modified electrodes: after electrodeposition, electrodes were cleaned carefully with distilled water and dried in air prior to use.

Electrochemistry. Voltammograms were acquired at 22 ± 2 °C with a CHI 760D electrochemical workstation (CH Instruments, Austin, Texas, USA) using a standard three-electrode electrochemical cell arrangement. For transient cyclic voltammetry, glassy carbon (3.0 mm diameter), Au (2.0 mm diameter), Pt (2.0 mm diameter) from CH Instruments (Austin, Texas, USA), ITO (Aldrich) or graphene modified working electrodes, a Pt wire counter electrode, and a Ag/AgCl (3 M NaCl) reference electrode (0.210 V vs SHE) were employed.[26] For rotating disk electrode (RDE) studies, a Rotating Ring Disk Electrode Rotator (RRDE-3A) (ALS Co., Japan) was connected to the electrochemical workstation. A GC disk (3.0 mm diameter, ALS Co., Japan) or a Pt disk (3.0 mm diameter, ALS Co., Japan) or graphene modified working electrode was used for RDE studies, along with the same reference and counter electrodes employed in the cyclic voltammetry. The bare working electrode in these and other experiments was polished, cleaned, sonicated, rinsed with water, and then dried under nitrogen. All solutions used in voltammetric experiments were purged with nitrogen for at least 15 min before measurements commenced, and then the electrochemical cell was kept under a positive pressure of nitrogen at all times. Simulations of the thin layer voltammograms were undertaken using the *Digisim* (v 3.05) software package.

Scanning Electron Microscopy (SEM). SEM images of the electrodeposited graphene film peeled off from an ITO electrode were obtained using a JEOL JEM 7001 FEGSEM field-emission instrument.

Raman Spectroscopy. Raman spectra of the electrodeposited graphene, graphene oxide, and graphite modified ITO were obtained using a Renishaw inVia Microscope.

RESULTS

Electrochemical and SEM Characterizations of Graphene Modified Electrodes. Electrochemical characterization of graphene modified electrodes was undertaken using cyclic voltammetry in an aqueous 0.50 M KCl electrolyte.

dx.doi.org/10.1021/la205013n | *Langmuir* 2012, 28, 5275−5285

Results with a graphene modified Pt electrode are shown in Figure 1a. Voltammetric data reveal that the capacitance current

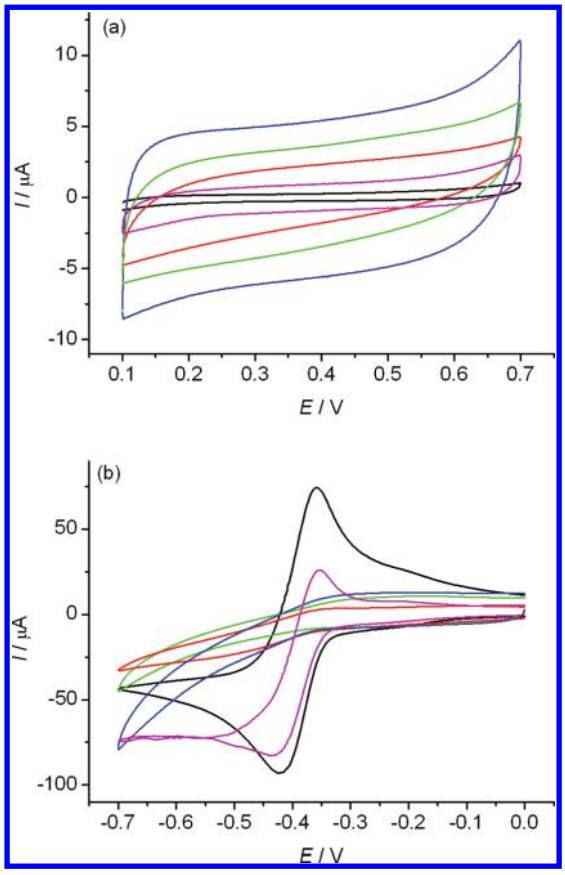

Figure 1. Cyclic voltammograms obtained from (a) a wet graphene modified Pt electrode in aqueous 0.50 M KCl electrolyte and (b) a wet graphene modified Pt electrode in an aqueous electrolyte containing 5.0 mM HCl and 0.50 M KCl. The modified electrode was fabricated by electrodeposition of graphene from graphene oxide solution by cycling the potential between 0 and −1.4 V vs Ag/AgCl (3 M NaCl) at a scan rate of 50 mV s^{-1} with a 2-mm-diameter Pt working electrode for 0 (black), 30 (magenta), 100 (red), 150 (green), and 200 (blue) cycles.

increases significantly when the deposition time increases, which suggests that the thickness of the graphene film also increases with deposition time. The fact that a large capacitance current is observed on graphene modified electrode, suggests that the electrodeposited graphene film is not highly compact (somewhat porous).

When preparing a graphene modified electrode, it is important to ensure that complete coverage of the conductive substrate with graphene is achieved so that the contribution from the underlying substrate is negligible. To verify that a full coverage of graphene is achieved, voltammograms of the H^+/H_2 process were recorded in an aqueous solution containing 5.0 mM HCl and 0.50 M KCl with a graphene modified Pt electrode. A highly characteristic chemically reversible H^+/H_2 process is obtained at a Pt electrode,[26,27] whereas the H^+ reduction process will be irreversible and occur at a more negative potential region if the surface is fully covered with graphene. The voltammogram in Figure 1b confirms that, at a bare Pt surface, a well-defined reversible H^+/H_2 process is observed with a midpoint potential (average of the reduction and oxidation peak potentials) of −0.390 V vs Ag/AgCl. As is also shown in Figure 1b, when the Pt surface is modified with graphene, the voltammetric characteristics gradually transform to those associated with a partially blocked surface.[28,29] This scenario gives rise to features associated with microelectrode array response at the uncovered Pt components of surface where radial diffusion contributes significantly to mass transport. When further graphene deposition is undertaken (Figure 1b), the overpotential for hydrogen ion reduction increases. Ultimately, the process becomes fully irreversible when more than 100 cycles of the potential are applied to achieve graphene deposition, which implies that the Pt substrate surface is now fully covered by graphene (Figure 1b).

Electrodeposition of graphene at GC, Au, or ITO electrodes appears to occur much more readily than at Pt as evidenced by the enhanced rate of increase in charging current (compare Figures S1 and 1a for the case of graphene modified Pt and GC electrodes). A thick graphene film electrodeposited onto an ITO electrode (100 cycles of potential) was peeled off the surface. SEM images derived from top and side of this film (Figure 2)

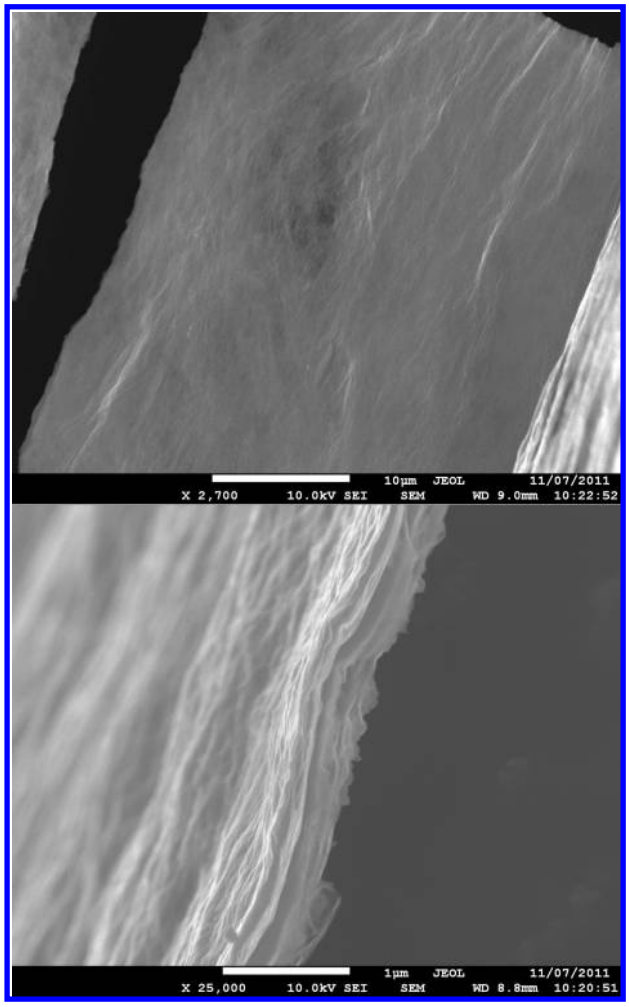

Figure 2. SEM images (top view and side view) of electrodeposited graphene film peeled off from an ITO electrode. The modified electrode was fabricated by electrodeposition of graphene from graphene oxide solution onto an ITO electrode by cycling the potential for 100 cycles between 0 and −1.4 V vs Ag/AgCl (3 M NaCl) in aqueous 0.05 M Na_2HPO_4 solution with an ITO electrode.

confirm that the graphene film is not flat and compact. Rather, there are significant gaps between the layers, and the structure should be porous to the electrolyte solution.

dx.doi.org/10.1021/la205013n | *Langmuir* 2012, 28, 5275−5285

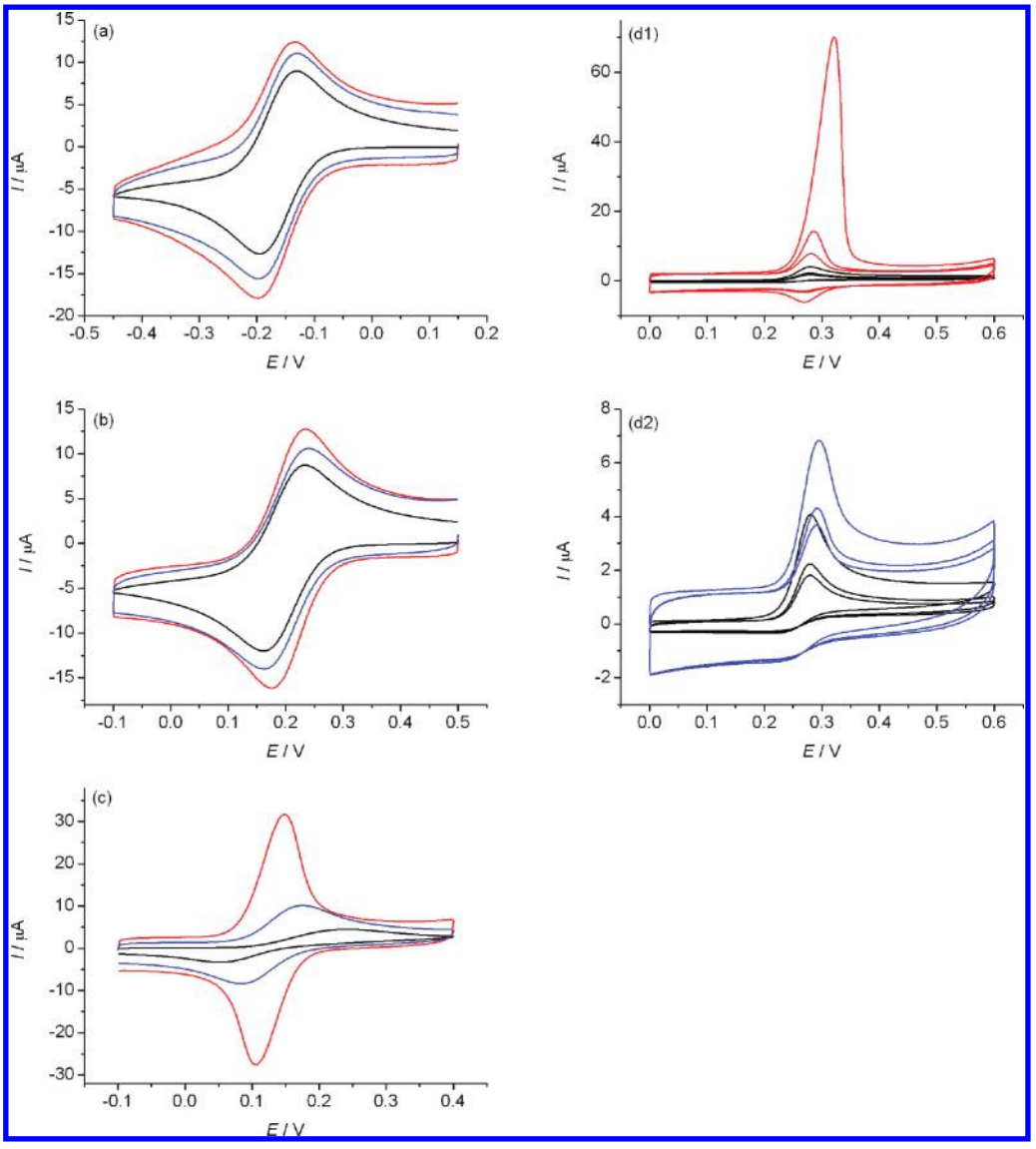

Figure 3. Cyclic voltammograms obtained using 3.0-mm-diameter GC (black), wet graphene modified (red), and dried graphene modified (blue) electrodes with a scan rate of 0.05 V s^{-1} in aqueous electrolyte solution containing (a) 1.1 mM $[Ru(NH_3)_6]^{3+}$ (0.1 M KCl), (b) 1 mM $[Fe(CN)_6]^{3-}$ (0.1 M KCl), (c) 0.2 mM hydroquinone (0.1 M sodium phosphate buffer, pH 6.0), and (d1,d2) 0.1 mM uric acid (0.1 M sodium phosphate buffer, pH 7.5) (d1: comparison of voltammograms obtained at bare GC electrodes (black) and wet graphene modified electrodes (red); d2: comparison of voltammograms obtained at bare GC (black) and dried graphene modified (blue) electrodes. The modified electrodes were fabricated by electrodeposition of graphene from graphene oxide solution by cycling the potential between 0 and −1.4 V vs Ag/AgCl at a scan rate of 0.05 V s^{-1} for 10 cycles while rotating the GC electrode at a rate of 104.7 rad s^{-1}.

Raman spectra of graphene films electrodeposited onto an ITO electrode were obtained using an excitation wavelength of 514.5 nm and show the characteristic G peak at ∼1590 cm^{-1}, the 2D peak at ∼2700 cm^{-1}, and the D peak located at ∼1350 cm^{-1} (Figure S2).[30]

Cyclic Voltammetry at Graphene Modified Electrodes. The voltammetry of the $[Ru(NH_3)_6]^{3+/2+}$ (eq 1) and $[Fe(CN)_6]^{3-/4-}$ (eq 2) processes, 1,4-hydroquinone (HQ) oxidation to 1,4-benzoquinone (BQ) (eq 3),[22] and uric acid (UA) oxidation (eqs 4 and 5)[31] processes was studied at both wet and dried graphene modified GC electrodes

$$[Ru(NH_3)_6]^{3+} + e^- \rightleftharpoons [Ru(NH_3)_6]^{2+} \quad (1)$$

$$[Fe(CN)_6]^{3-} + e^- \rightleftharpoons [Fe(CN)_6]^{4-} \quad (2)$$

$$HQ \rightleftharpoons BQ + 2e^- + 2H^+ \quad (3)$$

$$UA \rightleftharpoons \text{quinonoid diimine} + 2e^- + 2H^+ \quad (4)$$

$$\text{quinonoid diimine} \rightarrow \text{imine–alcohol} \quad (5)$$

For initial studies, a 3.0-mm-diameter graphene modified GC electrode was prepared by cycling the potential between 0 and −1.4 V (vs Ag/AgCl) under RDE conditions for 10 cycles to ensure a full coverage of graphene using the procedure described in the Experimental section. Cyclic voltammograms for the four processes of interest in this study with both wet and dried graphene modified and bare GC substrate electrodes are shown in Figure 3. Since the adsorption of analytes is likely to be favored at graphene modified electrodes, freshly prepared electrodes were used for each experiment.

dx.doi.org/10.1021/la205013n | *Langmuir* 2012, 28, 5275–5285

Table 1. Peak-to-Peak Separations and Background Corrected Peak Currents Obtained at Wet and Dried Graphene Modified and Bare GC Electrodes[a]

	ΔE_p (mV)[b]			peak current (μA)[b]		
process	bare GC	wet graphene	dried graphene	bare GC	wet graphene	dried graphene
$[Ru(NH_3)_6]^{3+/2+}$	66 ± 1	63 ± 1	67 ± 1	12.5 ± 0.2	15.7 ± 0.3	14.0 ± 0.3
$[Fe(CN)_6]^{3-/4-}$	71 ± 2	53 ± 2	80 ± 3	11.7 ± 0.3	14.3 ± 0.5	12.0 ± 0.4
HQ/BQ	190 ± 10	42 ± 2	92 ± 3	4.3 ± 0.1	28.9 ± 1.1	8.6 ± 0.3
UA oxidation	-	52 ± 2	-	3.9 ± 0.1	67.5 ± 4.1	5.4 ± 0.2

[a]Experimental conditions are as in the caption to Figure 3 [b]Measured from the first potential sweep.

As seen by perusal of Figure 3, the voltammograms obtained at wet and dried graphene modified electrodes and GC electrodes exhibit quite different characteristics. For example, cyclic voltammograms recorded at the wet graphene modified electrodes always exhibit higher background corrected currents and the separation between the reduction and oxidation peak potentials, ΔE_p values, are smaller for the chemically reversible $[Ru(NH_3)_6]^{3+/2+}$, $[Fe(CN)_6]^{3-/4-}$, and hydroquinone oxidation processes. Peak height and peak-to-peak separation data derived from the voltammograms in Figure 3 are summarized in Table 1.

The detection of large peak currents and smaller peak-to-peak separations, relative to those encountered at the substrate electrode, has frequently been used as evidence of higher activity of graphene modified electrodes,[5] based on the theories using a semi-infinite linear diffusion mass transport model.[28,32] However, careful analysis of the data in Table 1 suggests that some of the experimental observations are inconsistent with predictions based on linear diffusion. In addition to the diffusion component, thin layer, diffusion within pores,[17,19] and surface confined process from adsorbed species also may contribute to the total signal. The observations which support this postulate are as follows:

(i) The peak currents of all voltammograms recorded at graphene modified electrodes, except for the case of the $[Fe(CN)_6]^{3-/4-}$ process at a dried graphene modified electrode, are even higher than those predicted for either electrochemically reversible or quasi-reversible or chemically irreversible processes based on a semi-infinite linear diffusion mass transport model.[28] These larger than expected peak current values can be explained if there is an additional contribution to the diffusion component from other processes or the electrode is porous.

(ii) The peak-to-peak separation of 53 ± 2 mV for the $[Fe(CN)_6]^{3-/4-}$ process at a wet graphene modified GC electrode is even smaller than the theoretical value of 56.4 mV predicted under linear diffusion conditions for a fully reversible one-electron transfer process at 22 °C,[28] but is explicable in terms of peak separation with a contribution from a thin layer or surface confined process of adsorbed species, where the peak separation is predicted to be as small as zero for a reversible process.[28]

(iii) The shapes of the voltammograms, especially those in Figure 4c,d1 obtained with wet graphene modified electrodes for the oxidation of HQ and uric acid are closer to those predicted for a surface confined processes than a solution-phase process governed by semi-infinite linear diffusion.[28]

(iv) In the case of uric acid oxidation, the oxidation peak current obtained at a wet graphene modified GC electrode (Figure 3d1) is much larger and decreases much more rapidly on cycling of the potential than when a bare GC is used as the working electrode. Rapid depletion of uric acid is expected if uric acid is confined between graphene layers or adsorbed on graphene, as there is no continuous supply of uric acid available by diffusion within the graphene layers once it is irreversibly consumed by oxidation.

(v) Figure 3 reveals that voltammograms obtained with wet and dried graphene modified electrodes are distinctly different as expected if thin layer or surface confined processes contribute to the overall voltammetric response, which under this scenario is expected to be dependent on the geometric arrangement of the graphene layers.

(vi) A small reduction component is observed for uric acid oxidation process in Figure 3d1, which is consistent with previous findings by Shang et al.[33] Graphene prepared electrochemically from graphene oxide contains some functional groups, such as $-COO^-$, which may interact and stabilize the unstable quinonoid diimine formed upon oxidation of uric acid, as found with other biomolecules.[14]

RDE Voltammetry at Graphene Modified Electrodes. In principle, contributions to the transient voltamnmetry from all processes postulated to apply at a graphene modified electrode (diffusion, thin layer, surface confined) can be quantitatively calculated. Unfortunately, factors such as the exact geometric arrangement of graphene layers, the distribution of active sites and pores, and the adsorption isotherm to be applied (if adsorption occurs) are difficult to determine precisely. However, due to the lack of constant supply when the electroactive analyte is confined within graphene layers in either dissolved or adsorbed forms, these types of contribution to a voltammetric process will not reach steady state. In contrast, current magnitudes associated with solution-phase processes that occur at the outermost surface layer of graphene can reach steady state under rotating disk electrode conditions. Consequently, processes associated with the outermost graphene layer are expected to be dominant under RDE voltammertic conditions. In addition to this simplification, the inherently more favorable signal to charging current ratio available under steady-state voltammetric condition adds to the attractiveness of the RDE method for evaluation of voltammetry at graphene modified electrodes.

RDE voltammograms of all processes studied under transient conditions (Figure 3) were also obtained at wet and dried graphene modified GC electrodes, as well as at bare RDE GC electrodes (Figure 4). Again, freshly prepared graphene electrodes were used for each experiment to minimize the possibility of electrode contamination by adsorption. It should be noted that the double layer charging current of graphene modified electrodes is essentially unaffected by rotation (rotation rate $\leq$3000 rpm). This fact suggests that graphene modified electrodes are stable under hydrodynamic conditions of RDE employed in this study.

Importantly, the steady-state mass transport controlled limiting currents for all processes are now almost identical at both bare and graphene modified GC electrodes (Figure 4). This is expected

dx.doi.org/10.1021/la205013n | Langmuir 2012, 28, 5275−5285

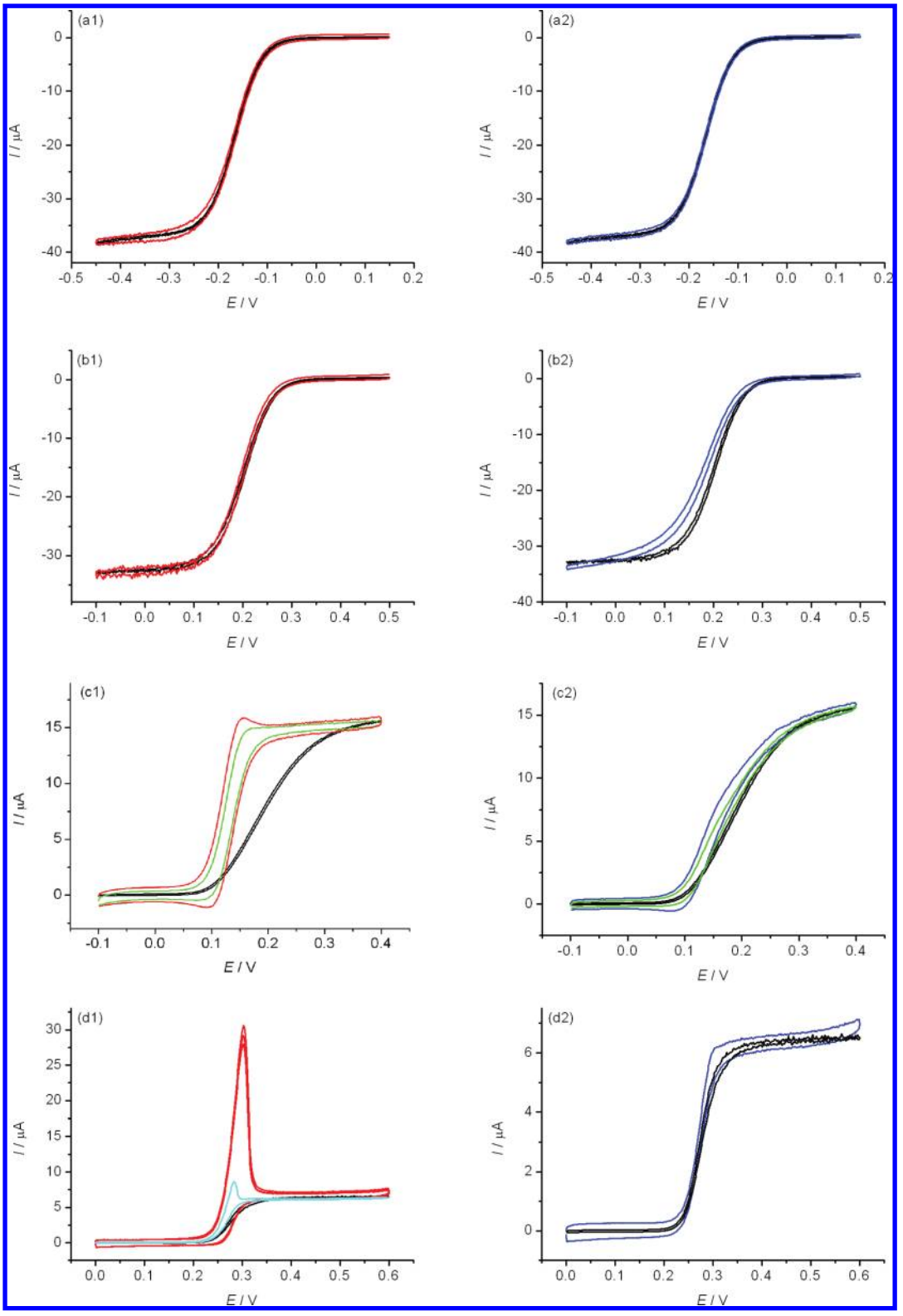

Figure 4. RDE voltammograms obtained using 3.0-mm-diameter GC (black), wet graphene modified (red), and dried graphene modified (blue) electrodes with a scan rate of 0.01 V s^{-1} and a rotation rate of 104.7 rad s^{-1} in aqueous solution containing (a) 1.1 mM $[Ru(NH_3)_6]^{3+}$ (0.1 M KCl), (b) 1 mM $[Fe(CN)_6]^{3-}$ (0.1 M KCl), (c) 0.2 mM hydroquinone (0.1 M sodium phosphate buffer, pH 6.0), and (d) 0.1 mM uric acid (0.1 M sodium phosphate buffer, pH 7.5). (a1−d1) Wet graphene (red, 0.01 V s^{-1}; green, 0.005 V s^{-1}; and cyan, 0.001 V s^{-1}) and bare GC (black, 0.01 V s^{-1}). (a2−d2) Dried graphene (blue, 0.01 V s^{-1}; and green, 0.005 V s^{-1}) and bare GC (black, 0.01 V s^{-1}). Deposition of graphene: 10 cycles of potential between 0 and −1.4 V (vs Ag/AgCl, 3 M NaCl) at a scan rate of 50 mV s^{-1}.

since the surface roughness of the electrode resulting from graphene modification should not affect the steady-state limiting current as long as the process remains mass-transport-controlled,[34] and other postulated non-mass-transport-controlled processes are

dx.doi.org/10.1021/la205013n | *Langmuir* 2012, 28, 5275−5285

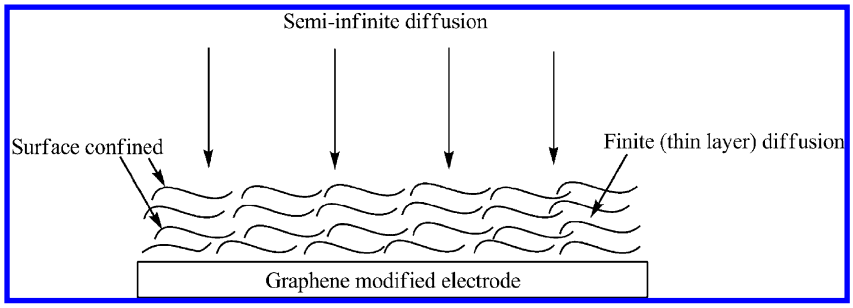

Figure 5. Schematic representation of the processes that may occur at a stationary graphene modified electrode.

no longer relatively significant. This outcome supports the hypothesis that the larger currents observed in transient voltammetry are associated with contributions from the processes that occur in addition to those governed by semi-infinite linear diffusion.

Voltammograms for the $[Ru(NH_3)_6]^{3+/2+}$ process obtained at all electrodes (Figure 4a1, a2) are essentially reversible. The heterogeneous charge transfer rate constant or k^0-value for the $[Ru(NH_3)_6]^{3+/2+}$ process is reported to be >0.2 cm s^{-1} at a GC macrodisk electrode[35] and >10 cm s^{-1} at nanoelectrodes,[36] implying conformance to Nernstian or reversible behavior under the experimental conditions used in this study.[20] RDE voltammetry could therefore appear to be insensitive to the kinetics even if a graphene modified electrode is more "active" than a bare GC electrode or vice versa, since the rate is likely to always remain fast enough for the process to be treated as electrochemically reversible. That is, $k^0 \gg 0.2$ cm s^{-1} at all electrode surfaces. A diffusion coefficient (D) of $(7.0 \pm 0.2) \times 10^{-6}$ cm^2 s^{-1} for $[Ru(NH_3)_6]^{3+}$ was calculated from the steady-state limiting current (I_L) based on the Levich relationship (eq 5). This value is in good agreement with the literature value of 6.7×10^{-6} cm^2 s^{-1}.[37]

$$I_L = 0.62nFAD^{2/3}\omega^{1/2}\nu^{-1/6}C^* \quad (5)$$

where n is the number of electrons transferred, F is Faraday's constant, A is the area of electrode, ω is the angular frequency of rotation, ν is the kinematic viscosity, and C^* is the bulk concentration of $[Ru(NH_3)_6]^{3+}$.

Even though the limiting current values are indistinguishable, the shapes and half wave potentials ($E_{1/2}$ − values) of voltammograms for the $[Fe(CN)_6]^{3-/4-}$ process obtained at a rotated dried graphene modified electrode differ from those obtained at rotated wet graphene modified or GC electrodes (Figures 4b1, b2). According to the theory for RDE voltammetry,[28,38] the fact that the slope of the voltammogram in the potential region near $E_{1/2}$ is significantly less steep implies that the k^0-value for the $[Fe(CN)_6]^{3-/4-}$ process is smaller at the dried graphene modified electrode. A D-value of $(7.2 \pm 0.2) \times 10^{-6}$ cm^2 s^{-1} for $[Fe(CN)_6]^{3-}$ was calculated from I_L and use of the Levich relationship (eq 5). This value is in close agreement with the literature value of 7.6×10^{-6} cm^2 s^{-1}.[28] At a dried graphene electrode, a heterogeneous charge transfer rate constant of 0.0085 cm s^{-1} and charge transfer coefficient of 0.45 were obtained from numerical simulation using the Butler–Volmer model of electron transfer and the following parameters: uncompensated resistance = 140 Ω, capacitance = 3×10^{-5} F, formal reversible potential = 0.201 V, and kinematic viscosity = 0.009 cm^2 s^{-1} for water[38] along with values of other parameters specified in the caption to Figure 4.

In the case of HQ oxidation, RDE voltammograms obtained at wet graphene modified electrodes exhibit a small peak prior to the convection controlled potential region when a rotation rate of 104.7 rad s^{-1} and an underlying dc scan rate of 10 mV s^{-1} is used (Figure 4c1). This component is attributed to the oxidation of adsorbed HQ,[39] and is nondetectable when a lower dc scan rate of 5 mV s^{-1} is applied (Figure 4c1). The slope of the current–potential (I/E) curve near $E_{1/2}$ is much steeper when a wet graphene modified electrode is used relative to the bare GC electrode case, suggesting that this modified electrode is more active for HQ oxidation based on use of the theory for RDE voltammetry.[28,38] In contrast, a dried graphene modified electrode does not exhibit evidence of superior activity toward the electrooxidation of HQ relative to a GC electrode, based on the RDE voltammetric data (Figure 4c2). However, these voltammograms exhibit wave splitting in the potential region close to $E_{1/2}$, suggesting that the reaction at this surface is more complicated than that described by eq 3, and may occur via two closely spaced one-electron steps. Nevertheless, again, the steady-state limiting currents obtained at the three types of electrode are comparable under all experimental conditions investigated. A diffusion coefficient (D) of $(8.8 \pm 0.3) \times 10^{-6}$ cm^2 s^{-1} for HQ was calculated from I_L based on the Levich equation and assuming the overall oxidation of HQ involves two electrons. The D value agrees well with that of 8.86×10^{-6} cm^2 s^{-1} reported in the literature in the same medium.[40] An unrealistically high D-value would be obtained if $n = 1$. Thus, it is concluded that HQ undergoes an overall two-electron oxidation in the pH 6.0 buffered aqueous medium used in this study, as proposed in eq 3.

RDE voltammograms for UA oxidation at wet graphene modified electrodes (Figure 4d1) show several of the characteristics noted for HQ oxidation. Thus, an even sharper oxidation component is present when the underlying dc scan rate is 10 mV s^{-1}. This peak is greatly diminished, but still detectable at a slow scan rate of 1 mV s^{-1}. Thus, adsorption of UA is assumed to be even more extensive than with HQ. However, the presumed adsorption component was not detected when a dried graphene modified electrode was used, even at a scan rate of 10 mV s^{-1} (Figure 4d2). The slope of the voltammogram near $E_{1/2}$ is steeper with a dried graphene modified electrode compared to the bare GC electrode (Figure 4d2). This suggests that dried graphene modified electrode is more active than the bare GC electrode toward the electrooxidation of UA under RDE conditions.[28,38] A D value of $(7.0 \pm 0.2) \times 10^{-6}$ cm^2 s^{-1} was calculated from I_L based on the Levich equation and assuming the overall oxidation of UA involves two electrons, again in excellent agreement with the value of 7.5×10^{-6} cm^2 s^{-1} reported by Huang et al.[41]

■ DISCUSSION

Experimental data imply that transient voltammetric responses obtained with graphene modified electrodes contain a significant

dx.doi.org/10.1021/la205013n | Langmuir 2012, 28, 5275–5285

additional contribution to the diffusion controlled Faradaic current from thin layer or adsorbed species. In principle, the total voltammetric Faradaic current may contain contributions from at least three sources. The relative contribution from each depends on the magnitude of the mass transport rate to the outermost surface layer of graphene, the surface chemistry associated with adsorption, and internally trapped material that depends on the thickness and geometric arrangement of graphene layers. Figure 5 shows a schematic diagram of the processes that may occur at a graphene modified electrode under stationary conditions. The model chosen is analogous to that used to describe transient voltammetry at carbon nanotube modified electrodes by Compton and co-workers.[17] In this situation, it is inappropriate to interpret the transient voltammetric data using the theories based solely on the semi-infinite linear diffusion mass transport model when the contributions from either thin layer or adsorbed species also are significant. Conclusions reached on the activity of graphene compared to other types of carbon electrodes that are based on transient voltammetry without taking into account the other contributions are likely to be incorrect or at least ambiguous.

The voltammetric theory for surface confined processes has been relatively well developed at stationary electrodes,[42] and is summarized in a comprehensive review article by Laviron.[42] In contrast, the theory for voltammetry in a thin layer and the effect of mass transport and the thickness of the thin layer is not highly developed. A schematic diagram of one thin layer cell configuration is provided in Figure 6. In this format, mass

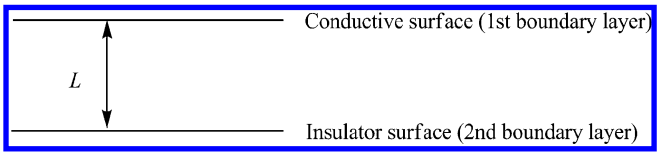

Figure 6. Schematic diagram of a thin layer cell (L is the thickness of the cell).

transport is blocked by the second boundary (flux of the electroactive analyte at this boundary is zero) and its concentration at the boundary layer is affected by depletion within the layer. For an ideal thin layer process, there is no concentration gradient within the layer. A stack of thin layer cells may be formed in a graphene modified electrode due to its layered structure (Figure 2). In this case, the first boundary layer is the surface of graphene. For convenience, the second boundary for each thin layer cell is set in the middle of two adjacent graphene layers where a zero flux boundary condition is applied as in conventional thin layer cell. Therefore, two classical thin layer cells are formed between two adjacent graphene layers. This formalism is adapted from that introduced by Compton and co-workers who considered the theory that applies for quasi-reversible electron transfer processes at carbon nanotuble modified electrodes.[17]

In experimental studies, the total response is the sum of all processes. The discussion below is limited to the predicted thin layer response based on the configuration in Figure 6, and the thin layer responses of three commonly encountered categories of reaction are examined. Numerical simulations using Digisim were undertaken and compared with voltammograms predicted when mass transport occurs by semi-infinite linear diffusion. The parameters used for the simulations are chosen to closely resemble those used experimentally in the studies with graphene modified electrodes. Thus, the diffusion coefficient was chosen to be 1.0×10^{-5} cm^2 s^{-1} for all species, the charge transfer coefficient α was assumed to be 0.5, $E^0 = 0$ V, the temperature was 295 K, the number of electrons transferred was 1, and the scan rate was around 0.1 V s^{-1}, with other parameters as specified below. For simplicity, effects of uncompensated resistance and capacitance were ignored in the simulations. In voltammograms presented (unless otherwise specified), the currents were normalized to the peak current to emphasize differences in the voltammetric features rather than absolute values of peak currents.

Reversible One-Electron Transfer Processes. The transient peak current (I_p) vs scan rate data (ν) are very often used to determine whether a reversible electron transfer process occurs in the solution phase ($I_p \propto \nu^{1/2}$), is a surface confined process or is an ideal thin layer process ($I_p \propto \nu$). The dependence of reduction peak current on $\nu^{1/2}$ (0.05 V s^{-1} $\leq \nu \leq$ 1 V s^{-1}) for both a reversible thin layer process with $L = 0.004$ cm and a reversible solution-phase process (semi-infinite linear diffusion) are compared in Figure 7. Voltammograms obtained

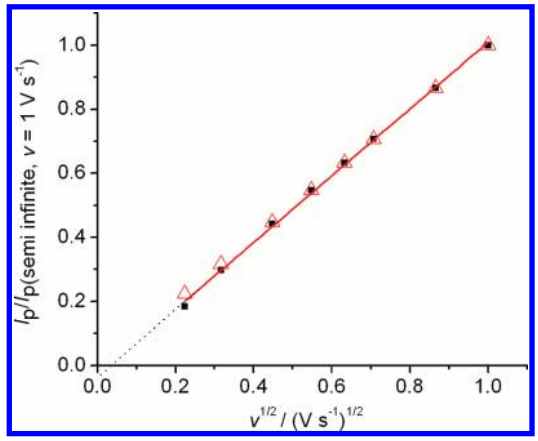

Figure 7. Dependence of simulated (L = 0.004 cm, other parameters as given in the text) peak currents on the square root of scan rate for a reversible one-electron thin layer process (■) and linear fit to data. Peak current data predicted for the semi-infinite linear diffusion case (△) are also provided for comparison. All peak currents are normalized with respect to the peak current for semi-infinite linear diffusion at a scan rate of 1 V s^{-1}.

with scan rates of 0.05 V s^{-1} and 1 V s^{-1} are shown in Figure S3 to demonstrate the effect of finite diffusion on voltammetric characteristics.

An almost perfect linear fit is obtained (Figure 7) for I_p versus $\nu^{1/2}$ (R^2 value of 0.999) even though voltammograms in Figure S3 show that finite diffusion has a significant effect on other voltammetric features, e.g., peak-to-peak separations and shapes, especially at slow scan rates. This outcome may be expected, since the presence of the second boundary has less effect on the peak current in the initial potential sweep normally used for scan rate dependent analysis. It may also be noted from examination of Figure 7 that there is a small negative intercept in the y (peak current) axis. This also is expected since the voltammograms obtained at higher scan rates are closer to that predicted for semi-infinite linear diffusion (Figure S3), where the presence of the second boundary has less effect on mass transport. Therefore, in the case of a graphene modified electrode, it is very difficult to rule out the presence of a contribution from thin layer effect based on the linear relationship between the peak current and the square root of scan rate, particularly

dx.doi.org/10.1021/la205013n | Langmuir 2012, 28, 5275−5285

given a significant level of experimental uncertainty. Although measurements undertaken with very slow scan rates may be helpful for identifying a contribution from a thin layer process, there are conditions where a larger contribution from radial diffusion will apply, further complicating the data analysis.

Quasi-Reversible One-Electron Transfer Processes. Normalized simulated voltammetric responses for the quasi-reversible Ox + $e^- \rightleftharpoons$ Red process with a k^0-value of 0.03 cm s^{-1} ($\alpha = 0.5$) are given for both semi-infinite linear diffusion and thin layer cases in Figure 8. The thickness (L) of the thin layer is

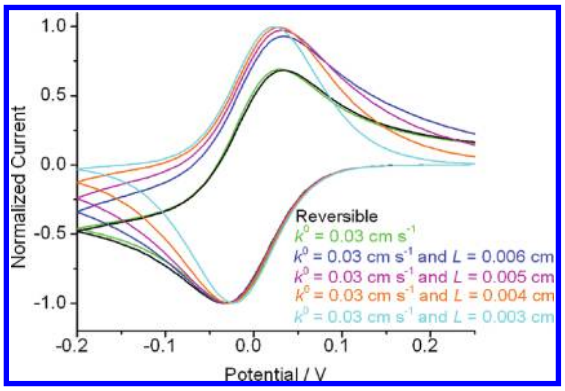

Figure 8. Normalized simulated quasi-reversible (k^0 = 0.03 cm s^{-1}, α = 0.5, scan rate = 0.1 V s^{-1}) voltammograms for a one-electron process with semi-infinite linear diffusion or finite diffusion (thin layer). Other parameters used in simulation are given in the text.

varied to show the predicted effect on the voltammetry. The ΔE_p values, summarized in Table 2, become smaller as the thickness of the thin layer decreases, as expected, due to an increase in depletion of analyte within the layers. Nevertheless, the voltammograms in Figure 8 still clearly include characteristics associated with transient voltammograms due to the contribution of semi-infinite linear diffusion within the layers. Thus, for a graphene modified electrode, unless contributions from thin layer and surface confined processes can be ruled out, it is not wise to conclude that graphene is more active than other carbon-type materials based on ΔE_p values and the application of the theory developed by Nicholson for the semi-infinite linear diffusion case.[32] The same conclusion was reached by Compton and co-workers in their studies on carbon nanotube modified electrodes.[17]

For an ideal thin layer process where mass transport plays no role, the voltammogram exhibits analogous characteristics predicted for a surface confined species with a Langmuir adsorption isotherm.[42] The rate constant of an ideal thin layer process (k^0_{tl}, with units of s^{-1} as for a surface confined process) can be calculated from eq 6 if the heterogeneous charge transfer rate constant (units of cm s^{-1}) is known,

$$k^0_{tl} = \frac{k^0}{L} \qquad (6)$$

Thus, it follows that k^0_{tl} increases as L decreases. In the case of a graphene modified electrode, k^0_{tl} will depend on the distance between adjacent graphene layers. Consequently, k^0_{tl} can depend on the method of modified electrode fabrication, even if k^0 remains unchanged. To illustrate the effect of L, voltammograms for the quasi-reversible process Ox + $e^- \rightleftharpoons$ Red simulated with $k^0 = 1.0 \times 10^{-6}$ cm s^{-1} and a range of L values are shown in Figure S4. Simulations clearly demonstrate that the separation between the oxidation and reduction peaks decreases as L decreases, which would lead to an increase in k^0_{tl} based on eq 6. Thus, again for a graphene modified electrode, conclusions of activity based on ΔE_p values, without taking into account the precise geometric arrangement of the graphene layers, are unwise, if a thin layer contribution is present.

Irreversible Processes. *Processes with Large Overpotential.* Processes such as oxygen reduction and hydrogen evolution are important in energy conversion. However, these and many others are usually very sluggish and hence require large overpotentials for the reactions to proceed at an appreciable rate. In order to improve their efficiency, catalysts are introduced to lower the overpotential and speed up the reaction. As a consequence, overpotential is often used as an indicator of the activity of the catalyst. Strictly speaking, the overpotential concept should apply when the rate is controlled by electron transfer, but in practice, the majority of processes are irreversible because of a coupled followup chemical reaction leading to the formation of an electro-inactive species (e.g., in the case of O_2 reduction to water) or the electrogenerated redox counterpart is electro-inactive (e.g., in the case of hydrogen ion reduction to hydrogen, hydrogen is inactive at most electrode materials within the potential window). Thus, in voltammetry, even though the peak potential is commonly used as an indication of reversibility, it does not necessarily have any direct thermodynamic significance.

Noting the above limitations on the significance of the overpotential concept, simulations of irreversible processes were undertaken to investigate the effect of a thin layer response on the voltammetric characteristics of irreversible processes, especially the peak potential. Simulated voltammograms for thin layer and semi-infinite diffusion cases derived for an electrochemically irreversible process of the kind Ox + $e^- \rightleftharpoons$ Red (E^0 = 0 V, $k^0 = 1.0 \times 10^{-7}$ cm s^{-1}), Red $\rightarrow$ Product (k_f = 100 s^{-1}), are provided in Figure 9. Clearly, in the thin layer case, the reduction peak shifts significantly to more positive potentials as the thin layer thickness decreases. It therefore follows that it is important to ensure that the contribution of thin layer processes is negligible when peak potentials obtained from cyclic voltammetry are used to evaluate the catalytic performance of a graphene modified electrode.

Chemically Irreversible Processes. The electrochemistry of many electroactive biologically important moieties, such as ascorbic acid, glucose, uric acid, and β-nicotinamide adenine dinucleotide, is chemically irreversible.[26] Simulations also were undertaken to investigate the effect of a thin layer response on the voltammetric characteristics of an electrochemically reversible but chemically irreversible process, Ox + $e^- \rightleftharpoons$ Red

Table 2. ΔE_p Values for Semi-Infinite Linear Diffusion and Thin Layer Cases for Simulated Voltammograms Presented in Figure 8

	semi-infinite linear diffusion		thin layer (k^0 = 0.03 cm s^{-1})			
mass transport model	k^0 = 0.03 cm s^{-1}	reversible	L = 0.006 cm	L = 0.005 cm	L = 0.004 cm	L = 0.003 cm
ΔE_p/mV	66.8	57.6	66.3	63.2	56.6	45.6

dx.doi.org/10.1021/la205013n | *Langmuir* 2012, 28, 5275–5285

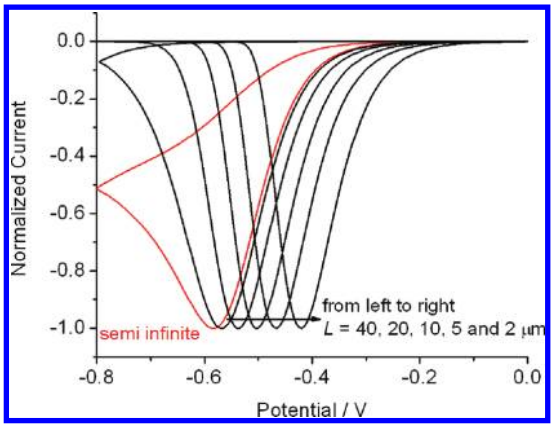

Figure 9. Normalized simulated voltammograms at a scan rate of 0.1 V s^{-1} for a fully irreversible process of the kind Ox + e^- ⇌ Red → Products, that is governed by semi-infinite linear diffusion (red) or finite diffusion (thin layer) (black). Parameters used in the simulation are given in the text.

(reversible electron transfer process with E^0 = 0 V), Red → Product (k_f = 100 s^{-1}). Results are shown in Figure S5 along with those for the semi-infinite linear diffusion case. In the thin layer case, multiple cycles of potential lead to a rapid decrease in peak current compared to the semi-infinite linear diffusion case (Figure S5) even though their voltammetric characteristics are similar in the first sweep of the potential. Rapid depletion of analyte confined within the layers causes the rapid decay of current on cycling the potential.

In the case of a graphene modified electrode, simulations yet again imply that it is difficult to deduce the activity of graphene based on peak potentials obtained from a cyclic voltammogram unless the absence of a contribution from a thin layer response can be confirmed. However, a contribution from a thin layer may be inferred by undertaking multiple cycles of the potential (Figure S5).

CONCLUSIONS

Graphene modified electrodes have been successfully fabricated by electrodeposition of graphene onto a conducting Pt, Au, glassy carbon, and indium tin dioxide substrates from an aqueous graphene oxide solution. Detailed voltammetric investigations of reversible $[Ru(NH_3)_6]^{3+/2+}$, quasi-reversible $[Fe(CN)_6]^{3-/4-}$, and irreversible hydroquinone oxidation and uric acid oxidation processes have been carried out at both bare and graphene modified GC electrodes using both transient (cyclic voltammetry) and steady-state (RDE) voltammetric techniques. Results imply that the voltammetric characteristics at graphene modified electrodes are complicated by a contribution from thin layer and surface confined adsorption processes. As a consequence, steady-state voltammetry at a rotating disk electrode affords a superior technique for the evaluation of the activity of graphene modified electrodes. The same situation should also prevail at other nanostructured electrodes with large surface area-to-volume ratio, if the contribution from thin layer and surface confined processes and double layer charging current can be reduced to a level where they are relatively unimportant. Experimental data with graphene modified electrodes prepared in this study also suggest that the contributions from surface confined and thin layer processes are strongly affected by the method of electrode fabrication, which determines the geometric arrangement of the graphene layers and the density of accessible active sites and porosity. Theoretical analysis using numerical simulation, as is the case with studies with carbon nanotube modified electrodes,[17] provides further insight into the implications on evaluation of the performance of graphene electrodes under conditions when contributions from the thin layer and surface confined processes are significant.

ASSOCIATED CONTENT

Supporting Information

Figures S1–S5, where Figure S1 contains a series of cyclic voltammograms illustrating the background current behavior of a wet modified graphene electrode, Figure S2 shows the Raman spectrum of graphene electrodeposited onto an ITO electrode, and Figures S3 to S5 represent simulated voltammograms used to illustrate outcomes of the theory contained in the text. This material is available free of charge via the Internet at http://pubs.acs.org.

AUTHOR INFORMATION

Corresponding Author

*E-mail: alan.bond@monash.edu; jie.zhang@monash.edu.

Notes

The authors declare no competing financial interest.

ACKNOWLEDGMENTS

Financial support from the Australian Research Council (LP100200206) and Aqua Diagnostic Ltd. is gratefully acknowledged. S.-F. Zhao thanks the China Scholarship Council for the award of funding to spend part of her PhD degree studies in Australia. The authors also thank Mr. Ling Qiu and the Monash Centre for Electron Microscopy for assistance in obtaining the SEM images.

REFERENCES

(1) Geim, A. K.; Novoselov, K. S. *Nat. Mater.* **2007**, *6*, 183–191.
(2) Rao, C. N. R.; Sood, A. K.; Subrahmanyam, K. S.; Govindaraj, A. *Angew. Chem., Int. Ed.* **2009**, *48*, 7752–7777.
(3) Novoselov, K. S.; Geim, A. K.; Morozov, S. V.; Jiang, D.; Zhang, Y.; Dubonos, S. V.; Grigorieva, I. V.; Firsov, A. A. *Science* **2004**, *36*, 666–669.
(4) Choucair, M.; Thordarson, P.; Stride, J. A. *Nat. Nanotechnol.* **2009**, *4*, 30–33.
(5) For recent review articles, see for example: (a) Ratinac, K. R.; Yang, W. R.; Gooding, J. J.; Thordarson, P.; Braet, F. *Electroanalysis* **2011**, *23*, 803–826. (b) Pumera, M. *Chem. Soc. Rev.* **2010**, *39*, 4146–4157. (c) Brownson, D. A. C.; Banks, C. E. *Analyst* **2010**, *135*, 2768–2778. (d) Chen, D.; Tang, L. H.; Li, J. H. *Chem. Soc. Rev.* **2010**, *39*, 3157–3180. (e) Shao, Y. Y.; Wang, J.; Wu, H.; Liu, J.; Aksay, I. A.; Lin, Y. H. *Electroanalysis* **2010**, *22*, 1027–1036.
(6) Li, W.; Tan, C.; Lowe, M. A.; Abruña, H. D.; Ralph, D. C. *ACS Nano* **2011**, *5*, 2264–2270.
(7) (a) Zhou, M.; Zhai, Y.; Dong, S. *Anal. Chem.* **2009**, *81*, 5603–5613. (b) Hallam, P. M.; Banks, C. E. *Electrochem. Commun.* **2011**, *13*, 8–11.
(8) Yang, S.; Xu, B.; Zhang, J.; Huang, X.; Ye, J.; Yu, C. *J. Phys. Chem. C* **2010**, *114*, 4389–4393.
(9) (a) Zhou, M.; Wang, Y.; Zhai, Y.; Zhai, J.; Ren, W.; Wang, F.; Dong, S. *Chem.—Eur. J.* **2009**, *15*, 6116–6120. (b) Shao, Y. Y.; Wang, J.; Engelhard, M.; Wang, C. M.; Lin, Y. H. *J. Mater. Chem.* **2010**, *20*, 743–748.
(10) Chen, L.; Tang, Y.; Wang, K.; Liu, C.; Luo, S. *Electrochem. Commun.* **2011**, *13*, 133–137.
(11) Goh, M. S.; Pumera, M. *Anal. Chem.* **2010**, *82*, 8367–8370.
(12) McCreery, R. L. *Chem. Rev.* **2008**, *108*, 2646–2687.

(13) Davies, T. J.; Hyde, M. E.; Compton, R. G. *Angew. Chem., Int. Ed.* **2005**, *44*, 5121−5126.
(14) Pumera, M.; Scipioni, R.; Iwai, H.; Ohno, T.; Miyahara, Y.; Boero, M. *Chem. Eur. J.* **2009**, *15*, 10851−10856.
(15) Ambrosi, A.; Bonanni, A.; Sofer, Z.; Cross, J. S.; Pumera, M. *Chem. Eur. J.* **2011**, *17*, 10763−10770.
(16) Buglione, L.; Chng, E. L. K.; Ambrosi, A.; Sofer, Z.; Pumera, M. *Electrochem. Commun.* **2012**, *14*, 5−8.
(17) Streeter, I.; Wildgoose, G. G.; Shao, L.; Compton, R. G. *Sens. Actuators, B* **2008**, *133*, 462−466.
(18) Hubbard, A. T.; Anson, F. C. *Electroanal. Chem.* **1970**, *4*, 129−210.
(19) Jones, C. P.; Jurkschat, K.; Crossley, A.; Compton, R. G.; Riehl, B. L.; Banks, C. E. *Langmuir* **2007**, *23*, 9501−9504.
(20) (a) Zhang, J.; Guo, S.-X.; Bond, A. M. *Anal. Chem.* **2007**, *79*, 2276−2288. (b) Sun, P.; Mirkin, M. V. *Anal. Chem.* **2006**, *78*, 6526−6534. (c) Muzikář, M.; Fawcett, W. R. *Anal. Chem.* **2004**, *76*, 3607−3611.
(21) Peter, L. M.; Durr, W.; Bindra, P.; Gerischer, H. *J. Electroanal. Chem.* **1976**, *71*, 31−50.
(22) (a) Ji, X.; Banks, C. E.; Silvester, D. S.; Wain, A. J.; Compton, R. G. *J. Phys. Chem. C* **2007**, *111*, 1496−1504. (b) White, J. H.; Soriaga, M. P.; Hubbard, A. T. *J. Electroanal. Chem.* **1985**, *185*, 331−338. (c) Parker, V. D. *Electrochim. Acta* **1973**, *18*, 519−524. (d) Hale, J. M.; Parsons, R. *Trans. Faraday Soc.* **1963**, *59*, 1429−1437.
(23) (a) O'Mullane, A. P.; Zhang, J.; Brajter-Toth, A.; Bond, A. M. *Anal. Chem.* **2008**, *80*, 4614−4626. (b) Shi, K.; Shiu, K.-K. *Electroanalysis* **2001**, *13*, 1319−1325. (c) Hsueh, C. C.; Brajter-Toth, A. *Anal. Chem.* **1993**, *65*, 1570−1575.
(24) Hummers, W. S. Jr.; Offeman, R. E. *J. Am. Chem. Soc.* **1958**, *80*, 1339−1339.
(25) Zhang, J.; Burt, D. P.; Whitworth, A. L.; Mandler, D.; Unwin, P. R. *Phys. Chem. Chem. Phys.* **2009**, *11*, 3490−3496.
(26) Sawyer, D. T.; Sobkowiak, A.; Roberts, J. L. *Electrochemistry for Chemists*, 2nd ed.; Wiley: New York, 1995.
(27) Zhang, J.; Ting, B.-P.; Khan, M.; Pearce, M. C.; Yang., Y. Y.; Gao, Z. Q.; Ying, J. Y. *Biosens. Bioelectron.* **2010**, *26*, 418−423.
(28) Bard, A. J.; Faulkner, L. R. *Electrochemical methods: fundamentals and applications*, 2nd ed.; Wiley: New York, 2001.
(29) (a) Amatore, C.; Saveant, J. M.; Tessier, D. *J. Electroanal. Chem.* **1983**, *147*, 39−51. (b) Brookes, B. A.; Davies, T. J.; Fisher, A. C.; Evans, R. G.; Wilkins, S. J.; Yunus, K.; Wadhawan, J. D.; Compton, R. G. *J. Phys. Chem. B* **2003**, *107*, 1616−1627. (c) Davies, T. J.; Moore, R. R.; Banks, C. E.; Compton, R. G. *J. Electroanal. Chem.* **2004**, *574*, 123−152. (d) Davies, T. J.; Banks, C. E.; Compton, R. G. *J. Solid State Electrochem.* **2005**, *9*, 797−808.
(30) (a) Zhu, Y.; Murali, S.; Cai, W.; Li, X.; Suk, J. W.; Potts, J. R.; Ruoff, R. S. *Adv. Mater.* **2010**, *22*, 3906−3924. (b) Ramesha, G. K.; Sampath, S. *J. Phys. Chem. C* **2009**, *113*, 7985−7989.
(31) (a) Owens, J. L.; Marsh, H. A.; Dryhurst, G. *J. Electroanal. Chem.* **1978**, *91*, 231−247. (b) Goyal, R. N.; Brajter-Toth, A.; Dryhurst, G. *J. Electroanal. Chem.* **1982**, *131*, 181−202. (c) Goyal, R. N.; Mittal, A.; Agarwal, D. *Can. J. Chem.* **1994**, *72*, 1668−1674. (d) Struck, W. A.; Elving, P. J. *Biochemistry* **1965**, *4*, 1343−1353.
(32) Nicholson, R. S. *Anal. Chem.* **1965**, *37*, 1351−1355.
(33) Shang, N. G.; Papakonstantinou, P.; McMullan, M.; Chu, M.; Stamboulis, A.; Potenza, A.; Dhesi, S. S.; Marchetto, H. *Adv. Funct. Mater.* **2008**, *18*, 3506−3514.
(34) Bruckenstein, S.; Sharkey, J. W.; Yip, J. Y. *Anal. Chem.* **1985**, *57*, 368−371.
(35) (a) Chen, P.; Fryling, M. A.; McCreery, R. L. *Anal. Chem.* **1995**, *67*, 3115−3122. (b) Jaworski, R. K.; McCreery, R. L. *J. Electroanal. Chem.* **1994**, *369*, 175−181.
(36) (a) Penner, R. A.; Heben, M. J.; Longin, T. L.; Lewis, N. S. *Science* **1990**, *250*, 1118−1121. (b) Sun, P.; Mirkin, M. V. *Anal. Chem.* **2006**, *78*, 6526−6534.
(37) Wipf, D. O.; Kristensen, E. W.; Deakin, M. R.; Wightman, R. M. *Anal. Chem.* **1988**, *60*, 306−310.
(38) Oldham, K. B.; Myland, J. C. *Fundamentals of Electrochemical Science*; Academic Press: San Diego, 1994.
(39) (a) Wang, Y.; Belding, S. R.; Rogers, E. I.; Compton, R. G. *J. Electroanal. Chem.* **2011**, *650*, 196−204. (b) Baltruschat, H.; Staud, N.; Heitbaum, J. *J. Electroanal. Chem.* **1987**, *239*, 361−374.
(40) Kaiser, T. J.; Thompson, J. W.; Mellors, J. S.; Jorgenson, J. W. *Anal. Chem.* **2009**, *81*, 2860−2868.
(41) Huang, X.; Im, H.; Yarimaga, O.; Kim, J.; Lee, D.; Kim, H.; Choi, Y. *J. Phys. Chem. B* **2006**, *110*, 21850−21856.
(42) Laviron, E. *Electroanal. Chem.* **1982**, *12*, 53−157.